

TWO SCENARIOS FOR BYPASS TRANSITION IN A BOUNDARY LAYER SUBJECTED TO A LOCALIZED PATCH OF DISTRIBUTED SURFACE ROUGHNESS

Aditya Anand

Department of Aerospace Engineering
Indian Institute of Science
Bangalore, 560012, India
adityaanand@iisc.ac.in

Sourabh S. Diwan

Department of Aerospace Engineering
Indian Institute of Science
Bangalore, 560012, India
sdiwan@iisc.ac.in

ABSTRACT

Here, we present two scenarios for bypass transition in a boundary layer downstream of a streamwise-localized patch of a distributed surface roughness. The two cases chosen for comparison (one at a relatively low speed and farther from the roughness, and the other at a higher speed but close to the roughness) are in the late stages of transition and have nominally similar Reynolds numbers and shape factors. However, the time-frequency behaviour, investigated using the Fourier and wavelet analysis, shows many contrasting features for the two cases. The pre-multiplied spectrum for the low-speed case shows a bimodal shape whereas that for the high-speed case is unimodal in shape. ‘Events’ are detected in the time-series for the wavelet coefficients for various frequencies. It is observed that for the low-speed case the wavelet events become increasingly more localized with increase in frequency whereas in the high-speed case the event intermittency remains constant over the entire frequency range. Furthermore, there seems to be a clustering of the events for the low-speed case, which can be identified with the turbulent spots in the velocity signal whereas no such clustering is observed for the high-speed case. The “spotty” transition observed for the low-speed case shares similarities with the bypass transition induced by freestream turbulence as well as the “natural” transition process. On the other hand, the “non-spotty” transition for the high-speed case seems to take a somewhat different transition route (in the late stages), wherein it proceeds without appearance of distinct turbulent spots. Such a scenario could have implications towards turbomachinery flow situations.

INTRODUCTION

The flow transition in a boundary layer in presence of elevated levels of background disturbances is termed “bypass” transition, as it bypasses the Tollmein-Schlichting route to turbulence (Morkovin, 1990). The bypass transition induced by free-stream turbulence (FST) has been

studied extensively in the past and has recently been reviewed by Zaki (2013) and Durbin (2017). The stages through which transition proceeds for this case has been well documented - the disturbances entering the boundary layer generate streamwise streaks, which undergo instability and breakdown into turbulent spots, which subsequently grow downstream and merge to form fully-turbulent boundary layer (Zaki, 2013). In fact, the final stage of bypass transition is quite similar to the final stage of “natural” transition, which also involves production, growth and merging of turbulent spots (Emmons, 1951; Narasimha, 1985).

There have also been studies on bypass transition induced by surface roughness in the form of a single roughness element or an array of roughness elements (e.g., Denissen & White, 2013). However, there have been limited measurements on bypass transition caused by a strip of distributed surface roughness. The early work on boundary-layer transition caused by a patch random distributed roughness (e.g., Von Doenhoff & Horton, 1958) was aimed at finding the critical Reynolds numbers (based on the roughness height) for the onset of transition. Interestingly, Von Doenhoff & Horton (1958) found that the streamwise extent of the roughened area did not have much effect on the critical Reynolds number. Corke et al. (1981) investigated the effect of extended surface roughness on the Tollmein-Schlichting as well as the bypass route to transition; see also the review article by Morkovin (1990). Pinson & Wang (2000) carried out measurements over a flat plate covered with two distributed-roughness scales to mimic the conditions present on a typical aero-engine turbine blade. They found that the step change between the two roughness grades played an important role in inducing early transition. The effect of random distributed roughness on the transient growth of disturbances was studied by Downs *et al.* (2008). They used localized patches of quasi-random rough surfaces arranged in the spanwise direction in the form of an array, with a smooth surface separating two consecutive patches. Downs *et al.* (2008) investigated three differ-

ent Reynolds numbers, each of which exhibited transient growth; the boundary-layer transition, however, was observed only for the highest Reynolds number. Zhang et al. (2018) carried out experiments over a localized forward/backward step (without any random roughness) covering the entire span of the plate and contrasted their results (using a conditional averaging technique) with those available in the literature on FST-induced transition. A transitional boundary layer downstream of a 2-D patch of distributed roughness, localized in the streamwise direction, was obtained in Diwan & Morrison (2017). They investigated the spectral structure of the boundary layer and its relevance to the spectral features in a fully-developed turbulent boundary layer.

Despite these studies, the exact transition mechanism in a boundary layer subjected to distributed roughness has not been studied in sufficient detail. Morkovin (1990) quotes a forthright comment by Eli Reshotko: “...our panel is in complete agreement namely that we are truly ignorant about bypass transition over surfaces with distributed roughness”. Although some progress has been made in the years following Morkovin’s review, basic questions like streak-formation mechanism and appropriate scaling for the roughness height in this type of transition are yet to be answered, as highlighted by Durbin (2017).

In this work we investigate bypass transition on a flat plate in presence of a two-dimensional localized patch of distributed roughness (similar to the one used in Diwan & Morrison, 2017). Two cases of transition are considered - one at a relatively low speed and second at a higher speed, both in the late stages of transition. We compare the two cases under similar conditions characterised by the shape factor and Reynolds number. The time-frequency behaviour of the velocity signals is analysed using the Fourier and wavelet transforms, and ‘events’ are detected in the wavelet time series using a certain threshold. We observe clustering of the events for the low-speed case over the entire high-frequency band, which can be identified with the turbulent spots in the velocity signal. On the other hand, for the high-speed case, no such clustering is observed and the events are distributed more evenly in time. While the transition process in the low-speed case shares similarities with the FST induced transition, the high-speed case seems to take on a somewhat different route, and proceeds without appearance of distinct turbulent spots. To the best of our knowledge, a non-spotty transition scenario in the late stages of bypass transition has not been reported in the literature so far.

EXPERIMENTAL ARRANGEMENT

Experiments are performed in an open circuit wind tunnel at the Indian Institute of Science Bangalore, with the test section size of 0.5m x 0.5m x 3m. The free stream turbulence intensity in the tunnel is about 0.1%. A flat plate with super-elliptic leading edge is mounted in the test section and a nominally zero pressure gradient is maintained over the length of the plate. Two configurations of surface roughness are used.

- Configuration A (CA) : A strip of distributed roughness (extra coarse emery sheet, grade 24) is pasted on the plate with its leading edge 100mm downstream of the plate leading edge and with the streamwise extent of 40mm (figure 1). The total roughness height (including the base of the emery sheet) is, $k=1.5\text{mm}$ and the roughness strip spans the entire width of the plate.

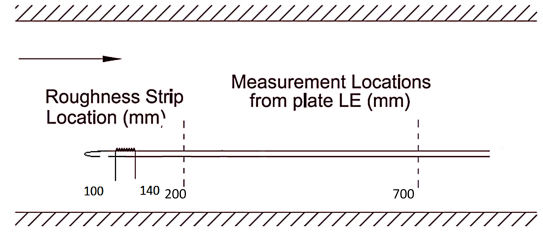


Figure 1. Schematic of the experimental setup

- Configuration B (CB) : Two roughness strips of a finer grade having streamwise extent of 20mm each are pasted on either sides of the roughness strip used in CA (not shown in figure 1), making the total length 80mm. This was done to make the change from the smooth to rough surface more gradual.

Most of the results presented in this paper are for CA, unless otherwise stated.

Velocity measurements are performed using a single-component constant-temperature hotwire anemometry (Streamline-Pro CTA from Dantec Dynamics). The hot-wire is calibrated against a Pitot tube using the Kings’ law. Temperature correction is applied to the hot-wire voltages to account for the tunnel temperature variation using

$$E_c = E \sqrt{\frac{T_w - T_r}{T_w - T_a}}, \quad (1)$$

where T_w is the wire temperature, T_r is the reference temperature, T_a is the ambient temperature, E is the measured voltage and E_c is the corrected voltage.

Power spectral densities for the measured velocity signals are calculated using the Welch’s periodogram method. The continuous wavelet analysis is carried out using the complex Morlet mother wavelet, as it gives a good compromise in terms of space and scale localization (Farge, 1992).

RESULTS AND DISCUSSION

Figure 2 shows the fluctuating velocity traces measured at $y/\delta = 0.1$ for $U_{fs} = 7.5$ m/s for four different streamwise (X) locations. Here U_{fs} is the freestream velocity and X is the distance from the plate leading edge. At $X = 300$ mm (figure 2a) the flow is pre-transitional and the first indications of the appearance of high-frequency fluctuations are seen at $X = 400$ mm (figure 2b). It is clear that the high frequencies cluster in the form of localized “turbulent spots”. Here we use the term turbulent spots in the sense it is defined in Emmons (1951) (see also Narasimha, 1985), i.e. as islands of turbulence in an otherwise laminar flow, which when detected using a hot-wire probe would appear as patches of high frequency fluctuation in the background laminar flow (figure 2b). In the present flow, the extent of the turbulent spots increases with distance as seen in figure 2c ($X = 450$ mm); however, they still retain their identity and are separated by near-laminar patches. At $X = 872$ mm the turbulent spots appeared to have merged indicating near-completion of the transition process. Thus, at $U_{fs} = 7.5\text{m/s}$, the roughness-induced bypass transition is qualitatively similar to the FST-induced transition, in that

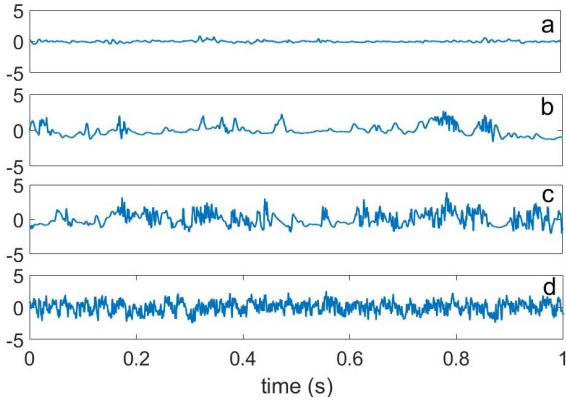


Figure 2. Fluctuating velocity traces at $y/\delta = 0.1$ for $U_{fs} = 7.5$ m/s at different streamwise locations. (a) $X = 300$ mm ($H = 2.44$), (b) $X = 400$ mm ($H = 2.18$) (c) $X = 450$ mm ($H = 1.97$) (d) $X = 872$ mm ($H = 1.48$). H is the shape factor. The y axis denotes the fluctuating velocity (m/s).

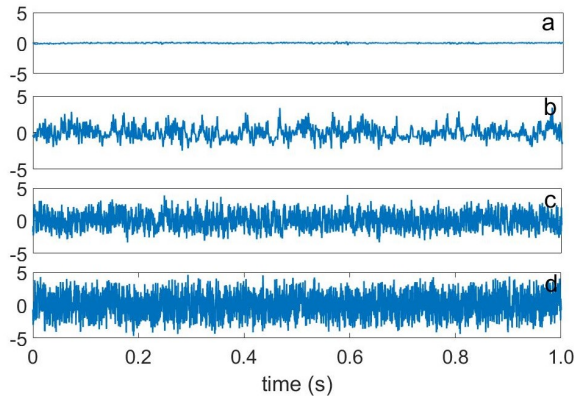


Figure 3. Representative fluctuating velocity traces at $X = 200$ mm for four different speeds: (a) $U_{fs} = 7.2$ m/s, (b) $U_{fs} = 8.5$ m/s, (c) $U_{fs} = 10.7$ m/s, (d) $U_{fs} = 16.6$ m/s. The y axis denotes the fluctuating velocity (m/s).

the transition proceeds through the generation and growth of turbulent spots.

It is conceivable that the same stages of transition as above would be observed in the velocity traces measured at a fixed streamwise station, sufficiently downstream of roughness strip, with gradual increase in the free-stream velocity (we have confirmed this behaviour although not shown here). Interestingly, a different behaviour in the velocity traces is observed when the hot-wire probe is placed fairly close to the roughness and the free-stream velocity is increased. Figures 3 (a)-(d) show the fluctuating velocity traces at $X = 200$ mm (i.e., 60 mm downstream of the trailing edge of the roughness strip) for four different free-stream velocities. At $U_{fs} = 7.2$ m/s (figure 3a), the flow is clearly pre-transitional. High frequency fluctuations are observed in figure 3(b) ($U_{fs} = 8.5$ m/s). Although we see some amplitude modulation of high-frequency fluctuations at this speed, the signal in figure 3(b) looks qualitatively different from those in figures 2(b) and (c). In other words, we do not see turbulent spots as per the definition of Emmons, i.e. islands in laminar flow, but rather the high-frequency fluctuations are present for most of the time interval (figure 3b). This behaviour is seen more clearly with further

increase in the free-stream velocity. Figures 3(c) and 3(d) correspond to $U_{fs} = 10.7$ m/s and 16.6 m/s respectively and there is no evidence of turbulence spots in both these signals, despite presence of high-frequency fluctuations.

The velocity signals in figures 3(c) and (d) look quite similar to those typically found in a fully-turbulent boundary layer. It was therefore of interest to determine the state of the boundary layer for these cases. Towards this, we measured a fully-developed turbulent boundary layer (TBL) in a separate experiment using a different tripping device at $Re_\theta = U_{fs}\theta/\nu = 2260$, where θ is the momentum thickness and ν is kinematic viscosity. The shape factor for the TBL was found to be 1.35, which is a typical value for a canonical TBL at moderate Reynolds number. The shape factors for the velocity profiles measured corresponding to the velocity signals in figures 3(c) and (d) are found to be 1.59 and 1.54 respectively, which are higher than $H = 1.35$ for the TBL. Furthermore, the rms intensity profiles of the fluctuating velocity for the two cases differ significantly from the profile for the TBL; see figure 4. This seems to suggest that the boundary layer at $X = 200$ mm for the two speeds $U_{fs} = 10.7$ m/s and 16.6 m/s is transitional in nature. Although this sounds reasonable, one needs to exercise caution as Purtell *et al.* (1981) have reported fully-developed TBLs at shape factors as high as 1.59 at $Re_\theta = 465$. Figure 4 includes the rms intensity profile for the TBL of Purtell *et al.* (1981) at $H = 1.52$ and $Re_\theta = 700$, which is comparable to $H = 1.54$ at $U_{fs} = 16.6$ m/s. First of all, the intensity profile for the TBL of Purtell *et al.* (1981) does not match with that for the TBL we have measured, presumably because of the difference in the Re_θ values for the two TBLs. More importantly, the rms intensity profiles for both the cases: $U_{fs} = 10.7$ m/s and 16.6 m/s at $X = 200$ mm, depart significantly from that of Purtell *et al.* (1981). The kind of departure we see here is similar to the one reported by Purtell *et al.* (1981) (figure 10 in their paper) for an “under-developed” TBL, which showed a slight departure from the fully-developed TBL data. Furthermore, they comment that the very low Reynolds-numbers for the TBL they studied implies that the flow is just beyond the transition from a laminar to a turbulent state. Thus any significant departure of the rms profiles from the fully-developed TBL profile at low Re_θ (as we see in figure 4) would mean the boundary layer is still in the transitional state and not yet fully turbulent. To lend further support to this argument we have included in figure 4, another rms profile at $U_{fs} = 12.6$ m/s for the second strip configuration- CB (see the previous section), with $H = 1.79$. This compares reasonably well with the two profiles for configuration- CA. The velocity traces for the boundary layer corresponding to CB (not shown here) did not show any evidence of turbulent spots and were found to be qualitatively similar those for CA shown in figures 3(c) and (d). As the shape factor for configuration- CB (1.79) is much higher than any TBL reported by Purtell *et al.* (1981), it is reasonable to conclude that this boundary layer is transitional in nature, although it does not show distinct turbulent spots. By implication we conclude that the two boundary layers ($U_{fs} = 10.7$ m/s and 16.6 m/s) for configuration- CA shown in figure 4 are also in transitional state.

Comparison between “spotty” and “non-spotty” transition scenarios

We have established above that the boundary layer at $X = 200$ mm and $U_{fs} = 16.6$ m/s (and 10.7 m/s) is transi-

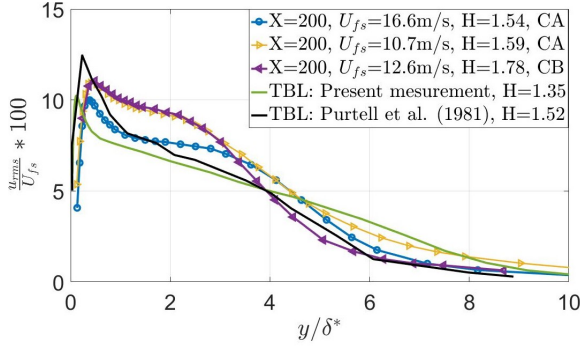


Figure 4. Comparison of turbulence intensity profiles in transitional boundary layers (configurations CA and CB) with those in the TBLs measured in this work and in Purtell *et al.* (1981).

tional, probably in its late stages, but does not show presence of turbulent spots - we call this “non-spotty” case of transition. On the other hand the boundary layer developing downstream at $U_{fs} = 7.5$ m/s shows distinct turbulent spots (figure 2), and we call this as a “spotty” case of transition. In particular we choose $X = 700$ mm at $U_{fs} = 7.5$ m/s (Case I) to compare with $X = 200$ mm and $U_{fs} = 16.6$ m/s (Case II). The relevant parameters for the two cases are listed in Table 1. As can be seen, the shape factor and the local Reynolds number for the two cases are quite similar and form the basis for comparison. The mean velocity and turbulence intensity profiles are shown in figure 5. Both profiles follow a similar trend for the two cases, although the turbulence intensities differ somewhat in magnitude.

The Reynolds number based on roughness height, $Re_k = \frac{U_{fs}k}{\nu}$ is around 639 and 1414 for Case I and II respectively. It is observed that the boundary layer immediately downstream of roughness for case I is in a pre-transitional state whereas for case II, transition has already been triggered at the roughness location. This is consistent with the critical Re_k for the onset of transition being 900 as proposed by Kraemer; see Schlichting & Gersten (1979); Von Doenhoff & Horton (1958) found the critical Re_k to be 680, which is still higher than the Re_k for case I. Another relevant parameter for a localized strip of roughness is the Reynolds number based on the streamwise extent of the roughness. However, we find this parameter to be relatively unimportant as can be seen by qualitative similar nature of transition at $X = 200$ mm for the two roughness configurations (figure 4), despite the fact that the roughness length for CB (although having two grades of roughness) is twice that of CA; see also Von Doenhoff & Horton (1958).

The qualitative differences in the velocity signal between Case I and II imply that there are differences between the two scenarios in terms of the time-frequency behaviour. The pre-multiplied Fourier spectrum gives the first clear evidence of structural differences between the two cases, as shown in figure 6. The spectrum for case I has a bi-modal shape with two distinct humps seen in the non-dimensional frequency-ranges ($f_n = \frac{f\delta}{U_{fs}}$) of $10^{-2} - 10^{-1}$ and $10^{-1} - 10^0$ respectively. On the other hand the spectrum for case II has a uni-modal shape with the spectral energy concentrated in the range $10^{-1} - 10^0$. This implies that there could be additional physical processes present for Case I (associated with the low-frequency hump) over and above those associated with the high-frequency hump which would be active

Table 1. Relevant parameters for the two comparison cases. δ : 99% thickness, δ^* : displacement thickness, $Re_{\delta^*} = \frac{U_{fs}\delta^*}{\nu}$, $Re_{\delta} = \frac{U_{fs}\delta}{\nu}$.

| Case | I (spotty) | II (non-spotty) |
|-----------------|------------|-----------------|
| $U_{fs}(m/s)$ | 7.5 | 16.6 |
| $X(mm)$ | 700 | 200 |
| $\delta(mm)$ | 13.8 | 5.5 |
| $\delta^*(mm)$ | 2.19 | 0.99 |
| $\theta(mm)$ | 1.41 | 0.64 |
| Re_{δ^*} | 939.2 | 943.6 |
| Re_{δ} | 5920.4 | 5247.5 |
| H | 1.55 | 1.54 |

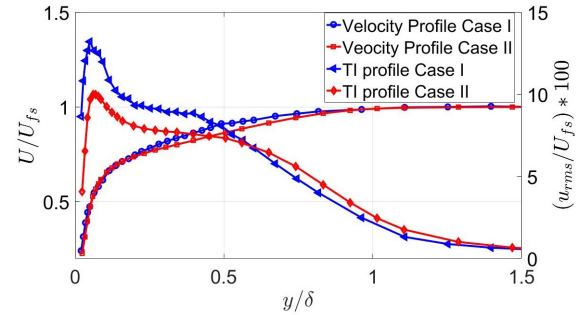


Figure 5. Mean velocity and turbulence intensity profiles for Cases I and II; see Table 1.

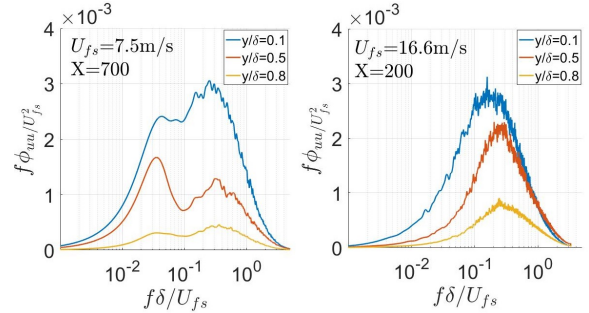


Figure 6. The pre-multiplied Fourier spectra for Case I (left panel) and Case II (right panel) at three wall normal locations.

in both of the cases.

The bi-modal structure in the pre-multiplied spectrum in a transitional boundary layer was also reported by Diwan & Morrison (2017), who used a roughness strip similar to that used in the present experiments. Diwan & Morrison (2017) attributed the presence of the low-frequency hump to the long streamwise streaks generated due to the interaction of the broad disturbance field generated by the roughness with the new internal boundary layer that would start downstream of roughness. Furthermore, they used Rapid Distortion Theory to give a theoretical explanation for the experimental observations. Based on their findings, the low

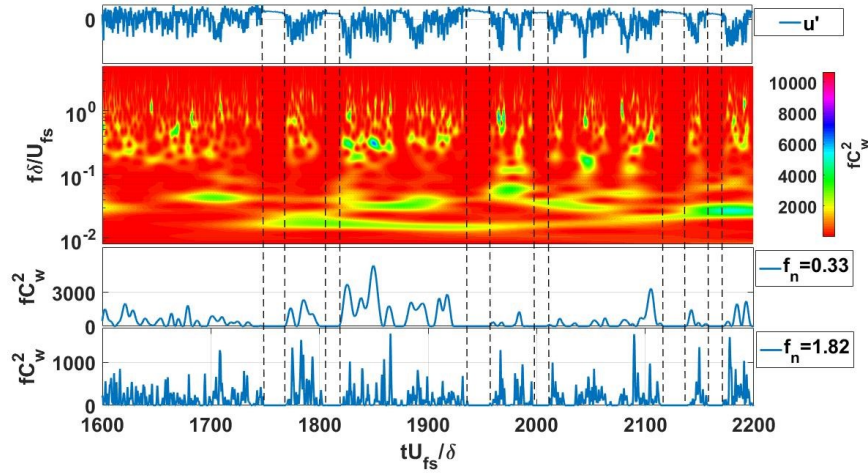


Figure 7. Wavelet analysis for Case I; Panel 1 : Fluctuating velocity signal, Panel 2 : Contour plot of pre-multiplied energy from wavelet coefficients, Panel 3 and 4 : pre-multiplied wavelet coefficients at $f_n = 0.33$ and 1.82 .

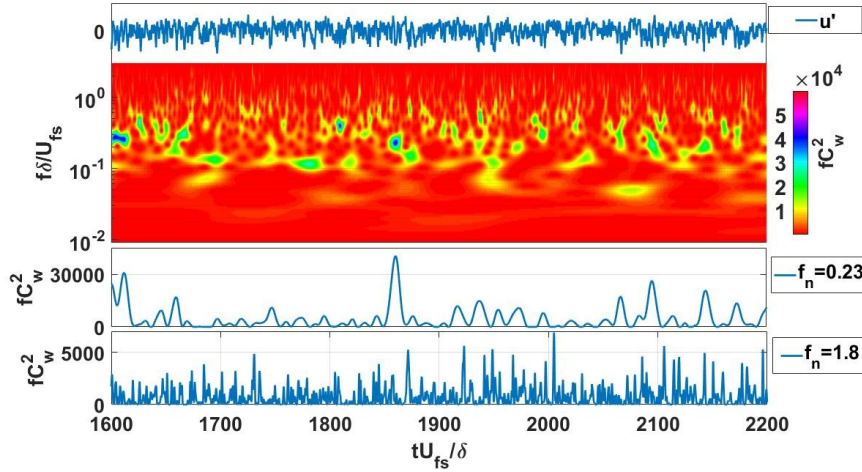


Figure 8. Wavelet analysis for Case II; Panel 1 : Fluctuating velocity signal, Panel 2 : Pre-multiplied contour plot of energy from wavelet coefficients, Panel 3 and 4 : pre-multiplied wavelet coefficients at $f_n = 0.23$ and 1.8 .

frequency hump observed in the bi-modal spectra for Case I in figure 6, could be associated with the presence of stream-wise streaks, which is the first stage of the “spotty” transition (Zaki, 2013). On the other hand, organized streaky structures seem to be absent for Case II as the spectral energy in the low-frequency band is negligible for this case (figure 6).

With an aim to establish a link between the absence of low-frequency spectral content and the non-spotty nature of the high speed case (Case II), we performed the continuous wavelet analysis. The results of the analysis are shown in figures 7 and 8. The first panel in each figure shows the velocity trace and the second panel shows the contour plot of the energy (amplitude squared: C_w^2) of the wavelet coefficients. We have used the pre-multiplied wavelet energy (fC_w^2) as the contour variable to enable a ready comparison with the pre-multiplied spectrum in figure 6. The concentration of energy in two frequency ranges for case I and that in only the high frequency range for case II is again evident from figures 7 and 8. What is also clear from the figures is that the energy at various frequencies is not uniformly present at all times but appears in localized patches for both the cases, indicating the intermittent nature of the transition process, which is a well-recognized aspect of bypass transi-

tion. However, the presence of intermittency in the wavelet time series does not imply occurrence of turbulent spots in the velocity signal. To understand this aspect, we take a closer look at the time-frequency behaviour, which reveals the subtle differences between the two cases.

Towards this, we use an ‘event’ detection scheme, inspired by the work of Kaspersen & Krogstad (2001), who used a method based on wavelets to detect burst events in a turbulent boundary layer. They detected events by locating peaks in wavelet coefficients along the dominant frequencies obtained from the spectra. We used a threshold of 10% of rms value of the pre-multiplied wavelet coefficients to detect the events, along the lines of Kaspersen & Krogstad (2001). The part of the time series above this threshold is defined as an ‘event’ and the part below the threshold is set to zero. The event chronicle for the wavelet coefficients thus obtained is presented in the third and fourth panels of figures 7 and 8 for two chosen frequencies. The energy contained in the events is about 85% of the total energy at each frequency. This fraction does depend upon the threshold used for event detection. However, the qualitative nature of the results would be unaffected even if a slightly different threshold is used.

Using the event chronicle the fractional time for which

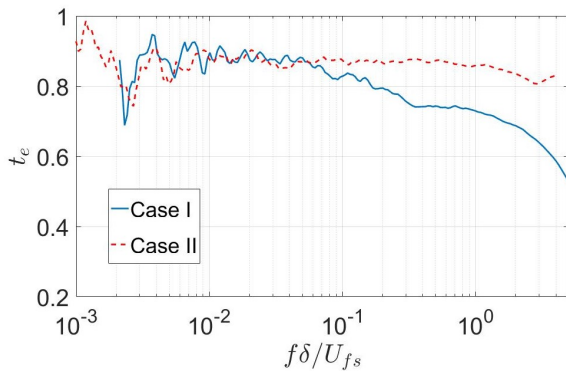


Figure 9. Fractional time for events (t_e) as a function of normalised frequency (f_n).

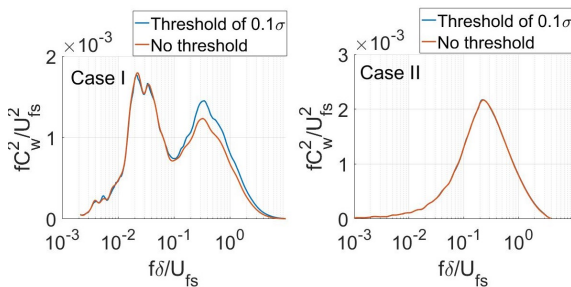


Figure 10. Comparison of the conditionally-averaged wavelet spectrum with the normal time-averaged spectrum.

the events are present (t_e) is calculated at each frequency and this is plotted in figure 9. For case I, t_e remains constant up to $f_n = 0.08$ beyond which it decreases with increasing frequency, whereas for case II, it remains more or less constant for the entire frequency range. This is reflected in the conditionally-averaged spectrum obtained from the wavelet coefficients (figure 10) showing higher energies in the frequency band $10^{-1} - 10^0$ for case I, whereas for case II no such enhancement is seen. This shows that the time localization of wavelet events increases with frequency for case I but not for case II, which is another important contrast between the two cases.

Finally, returning to figures 7 and 8, we see that there is a certain organisation of the wavelet events for case I, wherein the events are clustered together in groups over the high frequency band of $10^{-1} - 10^0$, which can be identified with the appearance of turbulence spots in the velocity signal interspersed by relatively idle (or near-laminar) periods (figure 7). For case II, however, no such organisation is evident in the wavelet events, which is consistent with the corresponding velocity signal which does not show any distinct turbulent spots (figure 8).

CONCLUSIONS

In this work we have investigated two bypass-transition scenarios, in the late stages of transition, for a boundary layer subjected to distributed surface roughness. Although the boundary layers for the two cases compared are at similar stages of transition (in terms of shape factor and Reynolds number) clear differences are observed in the

time-frequency behaviour of the velocity signals for the two cases. While the low-speed case represents a more common transition scenario involving appearance of turbulent spots (spotty transition), the high-speed case seems to take on a somewhat different transition route in which turbulent spots do not appear (non-spotty transition). In this work, we have found the non-spotty transition to occur for boundary layers with shape factors less than 1.8, i.e., corresponding to the late stages of transition. Whether turbulent spots would be present in the preceding stages of transition for this case is not yet clear. We plan to investigate this aspect in future.

ACKNOWLEDGEMENT

We acknowledge financial support from the Indian Institute of Science Bangalore towards carrying out the experiments.

REFERENCES

- Denissen, Nicholas A & White, Edward B 2013 Secondary instability of roughness-induced transient growth. *Phys. Fluids* **25** (11), 114108.
- Diwan, Sourabh S & Morrison, Jonathan F 2017 Spectral structure and linear mechanisms in a rapidly distorted boundary layer. *Int. J. Heat Fluid Flow* **67**, 63–73.
- Downs, Robert S, White, Edward B & Denissen, Nicholas A 2008 Transient growth and transition induced by random distributed roughness. *AIAA J.* **46** (2), 451–462.
- Durbin, Paul A 2017 Perspectives on the phenomenology and modeling of boundary layer transition. *Flow Turbul. Combust.* **99** (1), 1–23.
- Emmons, HW 1951 The laminar-turbulent transition in a boundary layer-part i. *J. Aero. Science* **18** (7), 490–498.
- Farge, Marie 1992 Wavelet transforms and their applications to turbulence. *Ann. Rev. Fluid Mech.* **24** (1), 395–458.
- Kaspersen, Jon Harald & Krogstad, Per-Åge 2001 Wavelet-based method for burst detection. *Fluid Dyn. Res.* **28** (3), 223.
- Morkovin, Mark V 1990 On roughness-induced transition: facts, views, and speculations. In *Instability and transition*, pp. 281–295. Springer.
- Narasimha, R 1985 The laminar-turbulent transition zone in the boundary layer. *Prog. Aerosp. Sci.* **22** (1), 29–80.
- Pinson, MW & Wang, T 2000 Effect of two-scale roughness on boundary layer transition over a heated flat plate: Part 2—boundary layer structure. *ASME J. Turbomach.* **122** (2).
- Purtell, LP, Klebanoff, PS & Buckley, FT 1981 Turbulent boundary layer at low reynolds number. *Phys. Fluids* **24** (5), 802–811.
- Schlichting, H & Gersten, K 1979 Boundary layer theory, mac graw hill. *New York*.
- Von Doenhoff, Albert E & Horton, Elmer A 1958 A low-speed experimental investigation of the effect of a sand-paper type of roughness on boundary-layer transition. *NACA Report 1349*.
- Zaki, Tamer A 2013 From streaks to spots and on to turbulence: exploring the dynamics of boundary layer transition. *Flow Turbul. Combust.* **91** (3), 451–473.